

Nonlinear Predictive Cost Adaptive Control of Pseudo-Linear Input-Output Models Using Polynomial, Fourier, and Cubic Spline Observables

Rami Abdulelah Alhazmi¹, Achinth Suresh Babu², Syed Aseem Ul Islam², and Dennis S. Bernstein²

Abstract—Control of nonlinear systems with high levels of uncertainty is practically relevant and theoretically challenging. This paper presents a numerical investigation of an adaptive nonlinear model predictive control (MPC) technique that relies entirely on online system identification without prior modeling, training, or data collection. In particular, the paper considers predictive cost adaptive control (PCAC), which is an extension of generalized predictive control. Nonlinear PCAC (NPCAC) uses recursive least squares (RLS) with subspace of information forgetting (SIFT) to identify a discrete-time, pseudo-linear, input-output model, which is used with iterative MPC for nonlinear receding-horizon optimization. The performance of NPCAC is illustrated using polynomial, Fourier, and cubic-spline basis functions.

I. Introduction

Aside from PID, the consensus of control practitioners is that model predictive control (MPC) is the most widely used and successful control technique [1]. MPC determines the control input by performing online, receding-horizon optimization, where a future sequence of control actions is determined, the first component of which is applied to the physical system, and the procedure repeats at subsequent steps. The success of MPC is due to its ability to stabilize, respect control constraints (e.g., magnitude and rate saturation), and enforce state constraints (e.g., safety limits on position and temperature) [2]–[6]. Although early applications of MPC focused on process control [7], the advent of fast embedded computing has extended the reach of MPC to aerospace systems [8].

For systems with linear dynamics, receding-horizon optimization can be performed using the backward propagating Riccati equation [4] or quadratic programming, where the latter can be used to enforce control and state constraints. For systems with nonlinear dynamics, various techniques have been developed for nonlinear MPC. For example, symbolic numerical differentiation is used in CasADi [9] together with iterative methods, such as interior-point methods [10], sequential quadratic

programming [11], [12], and quasi-linear parameter varying [13], [14].

MPC also lends itself to adaptive control, where system identification is performed concurrently online as a form of indirect adaptive control. This approach is embodied by generalized predictive control (GPC) [15]–[18], which uses MPC with online system identification performed by recursive least squares (RLS) with variable-rate forgetting (VRF). An extension of GPC is given by predictive cost adaptive control (PCAC) [19], where RLS is implemented with VRF to determine the need to accelerate learning. As shown in [19], PCAC benefits from self-generated persistency, thus avoiding the need for probing [20]. PCAC was applied experimentally in [21], [22] as well as numerically in [23], [24]. In many of these applications, PCAC is effective for nonlinear systems despite the fact that linear models are identified. Henceforth, in the present paper, we refer to PCAC as linear PCAC (LPCAC), to distinguish it from the nonlinear extension discussed below. For online nonlinear identification and MPC, Koopman approach is used in [25]–[27].

The goal of the present paper is to extend the effectiveness of LPCAC to more challenging nonlinear systems; this is done by identifying a nonlinear model and solving a nonconvex optimization problem. For nonlinear PCAC (NPCAC), we consider discrete-time, input-output models whose coefficients may depend on the output; these nonlinear systems are thus pseudo-linear systems as considered in [28]–[30]. For online system identification, NPCAC uses recursive least squares (RLS) with subspace of information forgetting (SIFT) to identify a discrete-time, pseudo-linear, input-output model [31]. For receding horizon optimization with discrete-time, pseudo-linear, input-output models, we use iterative model predictive control (IMPC) as described in [29], [32]. IMPC is chosen due to the fact that it is straightforward to implement and numerically reliable, at least for the examples considered in this paper. Since input-output models involve no internal state, NPCAC requires only the model outputs; hence, NPCAC is an adaptive output feedback controller. Finally, although NPCAC is based on discrete-time models, it can be applied to continuous-time systems under sampled data control as in the case of PCAC [19], [21]–[24].

¹This work was supported by King Fahd University of Petroleum and Minerals and NSF under grant CMMI 2310300.

¹Rami Abdulelah Alhazmi is with the Department of Aerospace Engineering, King Fahd University of Petroleum and Minerals, Dhahran, Saudi Arabia, and with the Department of Aerospace Engineering, University of Michigan, Ann Arbor, MI, USA rahaazmi@umich.edu

²Achinth Suresh Babu, Syed Aseem Ul Islam, and Dennis S. Bernstein are with the Department of Aerospace Engineering, University of Michigan, Ann Arbor, MI, USA {achinth, aseemisl, dsbaero}@umich.edu

II. Pseudo-Linear Input-Output System

The present paper considers the discrete-time pseudo-linear scalar input-output system

$$y_k = \sum_{i=1}^n -F_i(Y_{k-i:k-n})y_{k-i} + G_i(Y_{k-i:k-n})u_{k-i}, \quad (1)$$

where, for all $k \geq 0$, $y_k \in \mathbb{R}$ and $u_k \in \mathbb{R}$, $n \geq 1$ is the model order, and, for all $i = 1, \dots, n$,

$$Y_{k-i:k-n} \triangleq [y_{k-i} \ \dots \ y_{k-n}] \in \mathbb{R}^{1 \times (n+1-i)}, \quad (2)$$

$$F_i: \mathbb{R}^{1 \times (n+1-i)} \rightarrow \mathbb{R}, \quad G_i: \mathbb{R}^{1 \times (n+1-i)} \rightarrow \mathbb{R}. \quad (3)$$

III. Online Identification using RLS

Let $\hat{n} \geq 1$, $\ell_f \geq 1$, $\ell_g \geq 1$, $\ell_h \geq 1$, and, for all $k \geq 0$, let $\bar{F}_{1,k}, \dots, \bar{F}_{\hat{n},k} \in \mathbb{R}^{1 \times \ell_f}$, $\bar{G}_{1,k}, \dots, \bar{G}_{\hat{n},k} \in \mathbb{R}^{1 \times \ell_g}$, and $\bar{H}_k \in \mathbb{R}^{1 \times \ell_h}$ be the coefficient row vectors to be estimated using recursive least squares (RLS). Furthermore, for all $k \geq 0$, let $\hat{y}_k \in \mathbb{R}$ be an estimate of y_k defined by

$$\hat{y}_k \triangleq \sum_{i=1}^{\hat{n}} -\bar{F}_{i,k}f_{i,k}y_{k-i} + \bar{G}_{i,k}g_{i,k}u_{k-i} + \bar{H}_kh_k, \quad (4)$$

where, for $i = 1, \dots, \hat{n}$,

$$f_{i,k} \triangleq f_i(Y_{k-i:k-\hat{n}}) \in \mathbb{R}^{\ell_f}, \quad f_i: \mathbb{R}^{\hat{n}+1-i} \rightarrow \mathbb{R}^{\ell_f}, \quad (5)$$

$$g_{i,k} \triangleq g_i(Y_{k-i:k-\hat{n}}) \in \mathbb{R}^{\ell_g}, \quad g_i: \mathbb{R}^{\hat{n}+1-i} \rightarrow \mathbb{R}^{\ell_g}, \quad (6)$$

are vectors of basis functions, and

$$h_k \triangleq h(Y_{k-1:k-\hat{n}}) \in \mathbb{R}^{\ell_h}, \quad h: \mathbb{R}^{\hat{n}} \rightarrow \mathbb{R}^{\ell_h} \quad (7)$$

is a vector of basis functions. In the case where $h = 0$, for all $k \geq 0$ and all $i = 1, \dots, \hat{n}$, let $\hat{F}_{i,k}: \mathbb{R}^{1 \times \hat{n}+1-i} \rightarrow \mathbb{R}$ and $\hat{G}_{i,k}: \mathbb{R}^{1 \times \hat{n}+1-i} \rightarrow \mathbb{R}$ be approximate functions of F_i and G_i defined by

$$\hat{F}_{i,k}(Y_i) \triangleq \bar{F}_{i,k}f_i(Y_i), \quad \hat{G}_{i,k}(Y_i) \triangleq \bar{G}_{i,k}g_i(Y_i), \quad (8)$$

where $Y_i \in \mathbb{R}^{1 \times \hat{n}+1-i}$. For all $k \geq 0$, the pseudo-linear input-output (PLIO) model (4) can be written as

$$\hat{y}_k = \bar{\theta}_k\phi_k, \quad (9)$$

where

$$\bar{\theta}_k \triangleq [\bar{F}_{1,k} \ \dots \ \bar{F}_{\hat{n},k} \ \bar{G}_{1,k} \ \dots \ \bar{G}_{\hat{n},k} \ \bar{H}_k] \in \mathbb{R}^{1 \times \ell_\phi}, \quad (10)$$

$$\phi_k \triangleq \begin{bmatrix} -f_{1,k}y_{k-1} \\ \vdots \\ -f_{\hat{n},k}y_{k-\hat{n}} \\ g_{1,k}u_{k-1} \\ \vdots \\ g_{\hat{n},k}u_{k-\hat{n}} \\ h_k \end{bmatrix} \in \mathbb{R}^{\ell_\phi}, \quad \ell_\phi \triangleq \hat{n}(\ell_f + \ell_g) + \ell_h. \quad (11)$$

For online identification, RLS is used to estimate the coefficients of the input-output model (4). Specifically,

we use the subspace of information forgetting RLS (SIFT-RLS) proposed by [31]. The first step in SIFT-RLS is the information filtering, which consists of

$$\bar{y}_k = \begin{cases} y_k, & \|\phi_k\| \geq \sqrt{\varepsilon}, \\ 0, & \text{else,} \end{cases} \quad \bar{\phi}_k = \begin{cases} \phi_k, & \|\phi_k\| \geq \sqrt{\varepsilon}, \\ 0_{\ell_\phi \times 1}, & \text{else,} \end{cases} \quad (12)$$

where $\varepsilon > 0$ is a tuning parameter ensuring numerical stability. Then, the forgetting is applied to the information subspace. In other words, the forgetting is applied to the covariance subspace parallel to the direction of the regressor. That is

$$R_k = R_{k-1} - (1 - \lambda)R_k\bar{\phi}_k(\bar{\phi}_k^T R_k \bar{\phi}_k)^{-1}\bar{\phi}_k^T R_k, \quad (13)$$

$$\bar{P}_k = P_{k-1} + \frac{1 - \lambda}{\lambda}\bar{\phi}_k(\bar{\phi}_k^T R_k \bar{\phi}_k)^{-1}\bar{\phi}_k^T, \quad (14)$$

where $\lambda \in (0, 1]$ is the forgetting factor. Lastly, the update step consists of

$$R_{k+1} = \bar{R}_k + \bar{\phi}_k^T \bar{\phi}_k, \quad (15)$$

$$P_{k+1} = \bar{P}_k - \bar{P}_k \bar{\phi}_k (1 + \bar{\phi}_k^T \bar{P}_k \bar{\phi}_k)^{-1} \bar{\phi}_k^T \bar{P}_k, \quad (16)$$

$$\bar{\theta}_{k+1} = \bar{\theta}_k + (\bar{y}_k - \bar{\theta}_k \bar{\phi}_k) \bar{\phi}_k^T P_{k+1}. \quad (17)$$

We initialize with a coefficient matrix $\bar{\theta}_0 \in \mathbb{R}^{1 \times \ell_\phi}$, a positive definite covariance matrix $R_0 \in \mathbb{R}^{\ell_\phi \times \ell_\phi}$, and $P_0 \triangleq R_0^{-1}$. Note that $\bar{\theta}_{k+1}$, computed using (17), is available at step k , and thus, $\bar{F}_{1,k+1}, \dots, \bar{F}_{\hat{n},k+1}, \bar{G}_{1,k+1}, \dots, \bar{G}_{\hat{n},k+1}, \bar{H}_{k+1}$ are available at step k by the definition of $\bar{\theta}_k$ in (10). We define the one-step prediction error by $e_{p,k} \triangleq y_k - \bar{\theta}_k \phi_k$.

IV. Model Predictive Control

Let $\ell \geq 1$ be the preceding horizon number of steps, and for all $k \geq \hat{n}$ and $i = 1, \dots, \ell$, the predicted counterpart sequences of all signals are denoted by $\chi_{k|i} \triangleq \chi_{k+i}$, where $\chi_{k|i}$ is the value of a signal χ at step $(k+i)$, using the information available at step k . Then, at step $k \geq \hat{n}$, the model predictive control (MPC) optimizes a quadratic cost. The optimized cost is given by

$$J_k \triangleq \sum_{i=2}^{\ell+1} (r_{k|i} - y_{k|i})^T Q (r_{k|i} - y_{k|i}) + \sum_{i=1}^{\ell} u_{k|i}^T R u_{k|i}, \quad (18)$$

where $Q \in \mathbb{R}$ is the positive-semi-definite command-following weights, $R \in \mathbb{R}$ is the positive definite control weights, and, for all $i = 1, \dots, \ell$, $r_{k|i}$ is the command signal. The optimized cost (18) was subject to the identified model (4), and, for all $i = 1, \dots, \ell$, control magnitude saturation given by $u_{\min} \leq u_{k|i} \leq u_{\max}$, where $u_{\min}, u_{\max} \in \mathbb{R}$. Then, $u_{k+1} = u_{k|1}$. For $k = 1, \dots, \hat{n}$, u_{k+1} is sampled from $\mathcal{N}(0, \sigma_u)$, where $\sigma_u > 0$ is a tuning parameter. We assume for all $k \geq \hat{n}$, r_k is known to the controller. We define the command-following error by $e_{c,k} \triangleq r_k - y_k$.

A. MPC For Linear Models

Let, for $i = 1, \dots, \hat{n}$, $f_i = 1$, $g_i = 1$, and $h = 0$. Then, the identified model (4) is linear and a linear MPC solver can be used to compute u_{k+1} , such as in Linear PCAC (LPCAC).

B. MPC For Nonlinear Models

This section presents iterative model predictive control (IMPC) for controlling PLIO models. At step k , IMPC computes a sequence of control inputs and predicted outputs over the horizon of length $\ell \geq 1$. To do this, a subiteration is performed $j = 0, \dots, \nu$ times. At subiteration j , the state-dependent-coefficients (SDC's) are constructed using the predicted sequence of outputs and controls. For QP, the quadratic cost is minimized to obtain a predicted sequence of controls, which are used to construct a predicted sequence of outputs. Then, Boyden root-finding technique computes a new sequence of controls. Finally, the first component of the optimized sequence of controls is applied at step $k+1$.

1) Prediction over the Horizon: At step k , IMPC takes the measurements y_k and applied control u_k , and computes the next control u_{k+1} . Hence, IMPC timing takes into account the computational delay as shown in Figure 1.

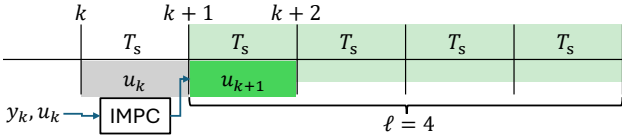


Fig. 1. Timing diagram for implementing IMPC at step k . At step k , IMPC uses y_k and u_k . Between steps k and $k+1$, u_k is applied and IMPC is executed and computes u_{k+1} . Between steps $k+1$ and $k+2$, u_{k+1} is applied. The green-shaded region shows the ℓ -step prediction horizon.

To compute u_{k+1} , we define the predicted output

$$\hat{y}_{k+1} \triangleq \bar{\theta}_{k+1} \phi_{k+1}. \quad (19)$$

Next, for all $k \geq 0$, $i = 1, \dots, \ell$, and $j = 0, \dots, \nu$, $\chi_{k|i,j}$ denotes the predicted value of χ_{k+i} at step k and subiteration j . Thus, for all $i = 2, \dots, \ell+1$ and $j = 0, \dots, \nu$, the predicted outputs are given by

$$y_{k|i,j} = \hat{\theta}_{k|i,j} \varphi_{k|i,j}, \quad (20)$$

where

$$\hat{\theta}_{k|i,j} \triangleq \begin{bmatrix} \tilde{F}_{1,k|i,j} & \dots & \tilde{F}_{\hat{n},k|i,j} & \tilde{G}_{1,k|i,j} & \dots & \tilde{G}_{\hat{n},k|i,j} & \tilde{H}_{k|i,j} \end{bmatrix} \in \mathbb{R}^{1 \times \ell_\varphi}, \quad (21)$$

$$\varphi_{k|i,j} \triangleq \begin{bmatrix} y_{k|i-1,j} & \dots & y_{k|\hat{n},j} & u_{k|i-1,j} & \dots & u_{k|\hat{n},j} & 1 \end{bmatrix}^\top \in \mathbb{R}^{\ell_\varphi}, \quad \ell_\varphi \triangleq 2\hat{n} + 1, \quad (22)$$

for all $i = 1, \dots, \hat{n}$,

$$\tilde{F}_{\iota,k|i,j} \triangleq -\hat{F}_{\iota,k}(Y_{k+i-\iota:k+i-\hat{n},j}), \quad (23)$$

$$\tilde{G}_{\iota,k|i,j} \triangleq \hat{G}_{\iota,k}(Y_{k+i-\iota:k+i-\hat{n},j}), \quad (24)$$

$$Y_{k+i-\iota:k+i-\hat{n},j} \triangleq [y_{k|i-\iota,j} \quad \dots \quad y_{k|\hat{n},j}], \quad (25)$$

for all $j = 0, \dots, \nu$, $y_{k|1,j} \triangleq \hat{y}_{k+1}$, for all $\iota = 0, \dots, \hat{n}-1$, $y_{k|-\iota,j} \triangleq y_{k-\iota}$, and

$$\tilde{H}_{k|i,j} \triangleq \bar{H}_{k+1} h(Y_{k+i-1:k+i-\hat{n},j}). \quad (26)$$

It thus follows from (20) that, for all $i = 2, \dots, \ell+1$, and $j = 0, \dots, \nu$,

$$y_{k|2,j} = \hat{\theta}_{k|2,j} \varphi_{k|2,j}, \quad (27)$$

⋮

$$y_{k|\ell+1,j} = \hat{\theta}_{k|\ell+1,j} \varphi_{k|\ell+1,j}. \quad (28)$$

Furthermore, we define the output, control, and command windows

$$Y_{k,j} \triangleq \begin{bmatrix} y_{k|2,j} \\ \vdots \\ y_{k|\ell+1,j} \end{bmatrix} \in \mathbb{R}^\ell, \quad U_{k,j} \triangleq \begin{bmatrix} u_{k|1,j} \\ \vdots \\ u_{k|\ell,j} \end{bmatrix} \in \mathbb{R}^\ell, \quad (29)$$

$$\mathcal{R}_k \triangleq \begin{bmatrix} r_{k|2} \\ \vdots \\ r_{k|\ell+1} \end{bmatrix} \in \mathbb{R}^\ell, \quad \mathcal{Y}_{k,j} \triangleq \begin{bmatrix} Y_{k,j} \\ U_{k,j} \end{bmatrix} \in \mathbb{R}^{2\ell}. \quad (30)$$

2) Cost and Constraints: We define the IMPC cost at step k

$$J_k(\mathcal{Y}) \triangleq \mathcal{Y}^\top \mathcal{H} \mathcal{Y} + \mathcal{F}_k^\top \mathcal{Y}, \quad (31)$$

where

$$\mathcal{H} \triangleq \text{diag}(I_\ell \otimes Q, I_\ell \otimes R) \in \mathbb{R}^{2\ell \times 2\ell}, \quad (32)$$

$$\mathcal{F}_k \triangleq \begin{bmatrix} -2(I_\ell \otimes Q)\mathcal{R}_k \\ 0_{\ell \times 1} \end{bmatrix} \in \mathbb{R}^{2\ell}, \quad (33)$$

$\mathcal{Y} \in \mathbb{R}^{2\ell}$ is the optimization variable.

The cost in (31) is subject to equality constraints that arise from (20). To formulate these constraints, we rewrite (27)–(28) as

$$Y_{k,j} = [F_{d,k,j} \quad G_{d,k,j}] D_k + F_{p,k,j} Y_{k,j} + G_{p,k,j} U_{k,j} + \bar{H}_{k,j}, \quad (34)$$

where

$$F_{d,k,j} \triangleq \begin{bmatrix} \tilde{F}_{\hat{n},k|2,j} & \dots & \tilde{F}_{1,k|2,j} \\ \vdots & \ddots & \vdots \\ 0 & \dots & \tilde{F}_{\hat{n},k|\hat{n}+1,j} \\ 0_{(\ell-\hat{n}) \times \hat{n}} & & & \end{bmatrix} \in \mathbb{R}^{\ell \times \hat{n}}, \quad (35)$$

$$G_{d,k,j} \triangleq \begin{bmatrix} \tilde{G}_{\hat{n},k|2,j} & \dots & \tilde{G}_{2,k|2,j} \\ \vdots & \ddots & \vdots \\ 0 & \dots & \tilde{G}_{\hat{n},k|\hat{n},j} \\ 0_{(\ell-\hat{n}+1) \times (\hat{n}-1)} & & & \end{bmatrix} \in \mathbb{R}^{\ell \times \hat{n}-1}, \quad (36)$$

$$D_k \triangleq [y_{k-\hat{n}+2} \ \cdots \ y_k \ \hat{y}_{k+1} \ u_{k-\hat{n}+2} \ \cdots \ u_k] \in \mathbb{R}^{2\hat{n}-1}, \quad (37)$$

$$F_{p,k,j} \triangleq \begin{bmatrix} 0 & \cdots & 0 & \cdots & 0 \\ \vdots & \ddots & \vdots & \ddots & \vdots \\ \tilde{F}_{\hat{n},k|\hat{n}+2,j} & \cdots & 0 & \cdots & 0 \\ \vdots & \ddots & \vdots & \ddots & \vdots \\ 0 & \cdots & \tilde{F}_{\hat{n},k|\ell+1,j} & \cdots & 0 \end{bmatrix} \in \mathbb{R}^{\ell \times \ell}, \quad (38)$$

$$G_{p,k,j} \triangleq \begin{bmatrix} \tilde{G}_{1,k|2,j} & \cdots & 0 & \cdots & 0 \\ \vdots & \ddots & \vdots & \ddots & \vdots \\ \tilde{G}_{\hat{n},k|\hat{n}+1,j} & \cdots & \tilde{G}_{1,k|\hat{n}+1,j} & \cdots & 0 \\ \vdots & \ddots & \vdots & \ddots & \vdots \\ 0 & \cdots & \tilde{G}_{\hat{n},k|\ell+1,j} & \cdots & \tilde{G}_{1,k|\ell+1,j} \end{bmatrix} \in \mathbb{R}^{\ell \times \ell}, \quad (39)$$

$$\bar{H}_{k,j} \triangleq [\tilde{H}_{k|2,j} \ \cdots \ \tilde{H}_{k|\ell+1,j}]^T \in \mathbb{R}^\ell, \quad (40)$$

Next, we write (34) as

$$A_{\text{eq},k,j} \mathcal{Y}_{k,j} = b_{\text{eq},k,j}, \quad (41)$$

where

$$A_{\text{eq}} \triangleq [I_\ell - F_{p,k,j} \ -G_{p,k,j}], \quad (42)$$

$$b_{\text{eq}} \triangleq [-F_{d,k,j} \ G_{d,k,j}] D_k + \bar{H}_{k,j}. \quad (43)$$

Thus, (31) is subject to

$$A_{\text{eq},k,j} \mathcal{Y} = b_{\text{eq},k}. \quad (44)$$

3) Optimization: At step k and at subiteration j , we minimize (31) subject to (44) using the MATLAB quadprog function with $\mathcal{Y}_{k,j}$ as the initial guess. We assume the SDC's (23), (24), and (26) are constant with respect to quadprog optimization. Hence, the constraints (44) is linear in $\mathcal{Y}_{k,j}$. Next, we define

$$Y_{k,j,\text{opt}} \triangleq [y_{k|2,j,\text{opt}} \ \cdots \ y_{k|\ell+1,j,\text{opt}}]^T \in \mathbb{R}^\ell, \quad (45)$$

$$U_{k,j,\text{opt}} \triangleq [u_{k|1,j,\text{opt}} \ \cdots \ u_{k|\ell,j,\text{opt}}]^T \in \mathbb{R}^\ell, \quad (46)$$

$$\mathcal{Y}_{k,j,\text{opt}} \triangleq [Y_{k,j,\text{opt}}^T \ U_{k,j,\text{opt}}^T]^T \in \mathbb{R}^{2\ell}, \quad (47)$$

where, for all $i = 1, \dots, \ell$ and $j = 0, \dots, \nu$, $y_{k|i+1,j,\text{opt}}$ and $u_{k|i,j,\text{opt}}$ are the minimizing outputs and controls at step k , respectively.

Lastly, we use Broyden method as described in [29] to accelerate the convergence of the subiteration and compute $U_{k|j+1}$.

Note, when the model (4) is linear, by setting f_i , g_i , and h as in subsection IV-A, we set $\nu = 1$, in which case IMPC is equivalent to LPCAC. Otherwise, we refer to IMPC as nonlinear PCAC (NPCAC).

V. Basis Functions

We approximate the nonlinearity in (1) using basis functions. The basis functions we consider in this paper are polynomial, Fourier, and cubic Hermite splines.

A. Polynomial Basis

The polynomial approximation of $f: [a, b] \rightarrow \mathbb{R}$ is

$$f(x) \approx c_1 + c_2 x + c_3 x^2 + \cdots + c_n x^n. \quad (48)$$

The basis functions are thus

$$b_{p,n}(x) \triangleq [1 \ x \ x^2 \ \cdots \ x^n]^T. \quad (49)$$

B. Fourier Basis

The Fourier approximation of $f: [-L, L] \rightarrow \mathbb{R}$ is

$$f(x) \approx a_0 + \sum_{i=1}^n \left[a_i \cos \frac{i\pi x}{L} + b_i \sin \frac{i\pi x}{L} \right]. \quad (50)$$

The basis functions are thus

$$b_{F,n}(x) \triangleq [1 \ \cos \frac{\pi x}{L} \ \sin \frac{\pi x}{L} \ \cdots \ \cos \frac{n\pi x}{L} \ \sin \frac{n\pi x}{L}]^T. \quad (51)$$

C. Cubic Hermite Spline

We use cubic Hermite splines for piecewise interpolation. The cubic Hermite spline approximation is $f: [s_0, s_{n+1}] \rightarrow \mathbb{R}$, where $n \geq 2$ is the number of equal segments. The nodes connecting all segments are s_0, \dots, s_{n+1} . We define the spacing $s_d \triangleq s_2 - s_1$. For all $i = 1, \dots, n$, we define two polynomial basis functions $p_i: [s_{i-1}, s_{i+1}] \rightarrow \mathbb{R}$ and $m_i: [s_{i-1}, s_{i+1}] \rightarrow \mathbb{R}$. The coefficient of p_i is associated with $f(s_i)$, which the other m_i is associated with $\frac{df}{dx}|_{s_i}$. For $i = 0, n+1$, we define $f(s_i) \triangleq 0$ and $\frac{df}{dx}|_{s_i} \triangleq 0$.

Then, for all $i = 1, \dots, n$, the i -th node basis functions are given by

$$b_i(x) \triangleq [p_i(x) \ s_d m_i(x)]^T, \quad (52)$$

where

$$p_i(x) \triangleq \begin{cases} 3t_i(x)^2 - 2t_i(x)^3, & s_{i-1} \leq x < s_i, \\ 1 - 3t_{i+1}(x)^2 + 2t_{i+1}(x)^3, & s_i \leq x < s_{i+1}, \\ 0, & \text{else,} \end{cases} \quad (53)$$

$$m_i(x) \triangleq \begin{cases} -t_i(x)^2 + t_i(x)^3, & s_{i-1} \leq x < s_i, \\ t_{i+1}(x) - 2t_{i+1}(x)^2 + t_{i+1}(x)^3, & s_i \leq x < s_{i+1}, \\ 0, & \text{else,} \end{cases} \quad (54)$$

and $t_i(x) \triangleq \frac{x-s_{i-1}}{s_d}$. Therefore,

$$f(x) \approx \sum_{i=1}^n [c_{i,1} \ c_{i,2}] b_i(x). \quad (55)$$

The basis functions are thus

$$b_{c,n}(x) \triangleq [b_1(x)^T \ \cdots \ b_n(x)^T]^T \in \mathbb{R}^{2n}. \quad (56)$$

VI. Numerical Examples with LPCAC

For the following two examples, LPCAC is applied to nonlinear systems. These examples are chosen to be challenging for LPCAC, thus setting the stage for NPCAC in the next section. For these examples, we set $f_1 = 1$, $g_1 = 1$, and $h = 0$, which makes (4) linear.

For all examples in this and the next section, let $y_0 = 0.1$, $u_0 = 0$, $\varepsilon = 1e-4$, $\sigma_u = 0.01$, $u_a = 0.1$, $Q = 1$, and the command signal $r_k \triangleq \pi \sin(\psi k)$, where $\psi \triangleq 0.05$ rad/step. For simplicity, magnitude saturation is not applied, and thus the control input is unconstrained.

Example 1. Consider (1), where

$$F_1 \triangleq -1.1, \quad G_1(y_{k-1}) \triangleq 0.9 + 0.5 \tan(y_{k-1}). \quad (57)$$

Note that (1) with (57) is unstable. We set $\bar{\theta}_0 = [1 \ 0.01 \ 0.01]$, $\lambda = 0.1$, $R_0 = 1e-3$, $\ell = 10$, and $R = 1e-2$. Figure 2 shows the command-following error. Figure 3 compares the estimated coefficients $\hat{G}_{1,k}(y_{k-1})$ with $G_1(y_{k-1})$ and shows the one-step prediction error. \diamond

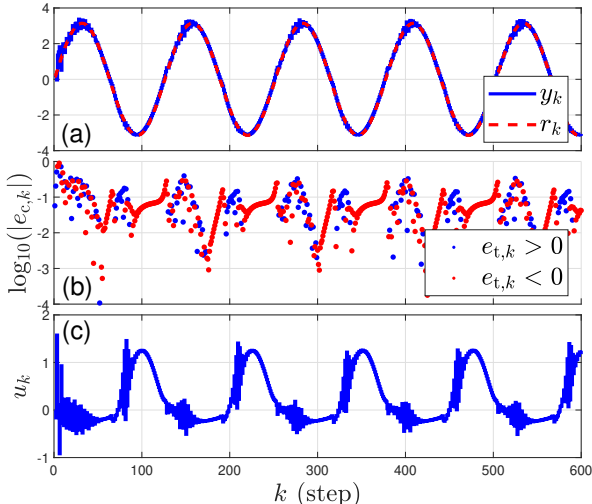


Fig. 2. Example 1: LPCAC of (57). (a) shows the measurement y_k and the command r_k ; (b) shows the command-following error $\log_{10}(|e_{c,k}|)$; (c) shows the control u_k .

Example 2. Consider (1), where

$$F_1 \triangleq -1.1, \quad G_1(y_{k-1}) \triangleq 0.4 + 0.5 \tan(y_{k-1}), \quad (58)$$

which is identical to (57) except that 0.9 is replaced by 0.4, in which case $G_1(y_{k-1})$ can become zero and change sign during operation. We choose $R = 1$. We set $\bar{\theta}_0$, λ , ℓ , and R_0 . Figure 4 shows the command-following error. Figure 5 compares the estimated coefficients $\hat{G}_{1,k}(y_{k-1})$ with $G_1(y_{k-1})$ and shows the one-step prediction error. \diamond

It may be conjectured that the poor performance of LPCAC shown in Figure 4 is at least partly due to the fact that, when $G_1(y_{k-1})$ in (58) becomes zero, control authority is lost. In the next section, we show that, despite the sign change in $G_1(y_{k-1})$ in (58), NPCAC has much better performance than LPCAC.

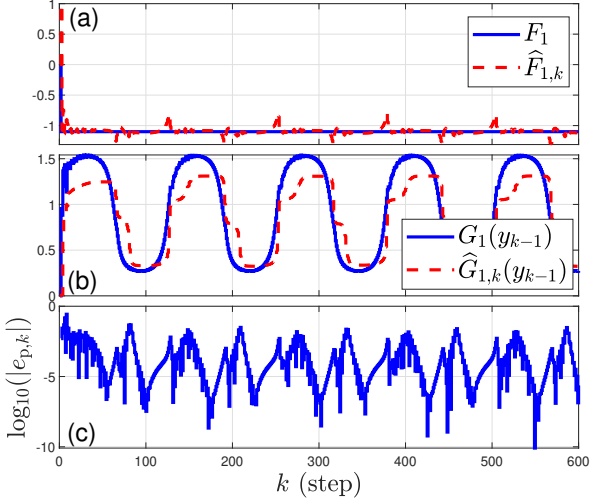


Fig. 3. Example 1: LPCAC of (57). (a) shows F_1 and its estimate $\hat{F}_{1,k}$; (b) shows $G_1(y_{k-1})$ and its estimate $\hat{G}_{1,k}(y_{k-1})$; (c) shows the one-step prediction error $\log_{10}(|e_{p,k}|)$.

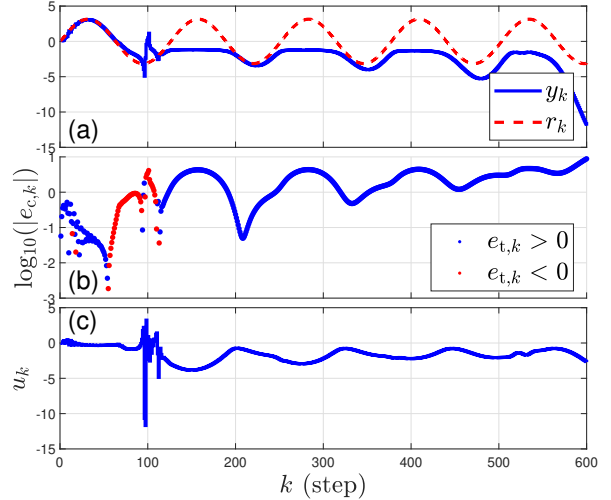


Fig. 4. Example 2: LPCAC of (58). (a) shows the measurement y_k and the command r_k ; (b) shows the command-following error $\log_{10}(|e_{c,k}|)$. (c) shows the control u_k . Note that the command-following error is an order of magnitude higher than in Example 1.

VII. Numerical Examples with NPCAC

For the following three examples, NPCAC is applied to nonlinear systems. As a baseline (BL) result, the nonlinear coefficient in the nonlinear system is included as a basis. The BL is compared with the n -element polynomial basis (PB n), the n -element Fourier basis (FB n), and the n -element cubic-spline basis (CB n). For all examples, we set $h = 0$, $\nu = 10$, and $\ell = 20$.

Example 3. Consider (58). For BL, we choose $f_1 = 1$ and $g_1(y_{k-1}) = [1 \ \tan y_{k-1}]^T$. We set $\bar{\theta}_0 = [1 \ 0.01 \ 0.01]$, $\lambda = 0.1$, $R_0 = 1e-3$, and $R = 0$. For PB2, we choose $f_1 = 1$ and $g_1(y_{k-1}) = b_{p,1}(y_{k-1})$. We set $\bar{\theta}_0 = [1 \ 0.01 \ 0.01]$, $\lambda = 0.1$, $R_0 = 1e-2$, and $R = 2e-4$. For FB3, we choose $f_1 = 1$ and $g_1(y_{k-1}) = b_{f,1}(y_{k-1})$, where $L = 6$. We set $\bar{\theta}_0 = [1 \ 0.01 \ 0.01 \ 0.01]$, $\lambda = 0.3$, $R_0 = 1e-1$, and $R = 4e-3$. For CB4, we choose

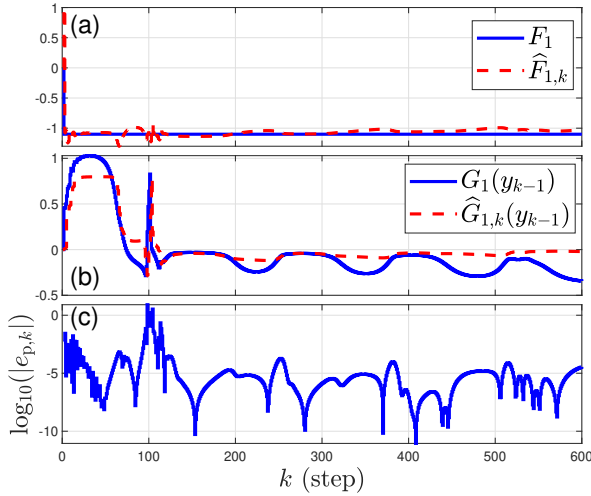


Fig. 5. Example 2: LPCAC of (58). (a) shows F_1 and its estimate $\hat{F}_{1,k}$; (b) shows $G_1(y_{k-1})$ and its estimate $\hat{G}_{1,k}(y_{k-1})$; (c) shows the one-step prediction error $\log_{10}(|e_{p,k}|)$. Note that unlike Figure 3(b) in Example 1, $G_1(y_{k-1})$ crosses zero.

$f_1 = 1$, and $g_1(y_{k-1}) = b_{c,2}(y_{k-1})$, where $s_0 = -6$ and $s_3 = 6$. We set $\bar{\theta}_0 = [1 \ 0.01 \ 0.01 \ 0.01 \ 0.01]$, $\lambda = 0.1$, $R_0 = 1e-3$, and $R = 7e-4$.

Figure 6 compares the command-following error and the one-step prediction error for BL, PB2, FB3, and CB4. Figure 7 compares the estimated coefficient $\hat{G}_{1,450}(y)$ with $G_1(y)$ for BL, PB2, FB3, and CB4. Figure 8 shows the estimated coefficients $\bar{F}_{1,k}$ and $\bar{G}_{1,k}$ for PB2. Figure 9 shows the measurement y_k , the command r_k , and the control u_k for CB4. Figure 10 compares the estimated coefficients $\hat{G}_{1,k}(y_{k-1})$ with $G_1(y_{k-1})$ for CB4. \diamond

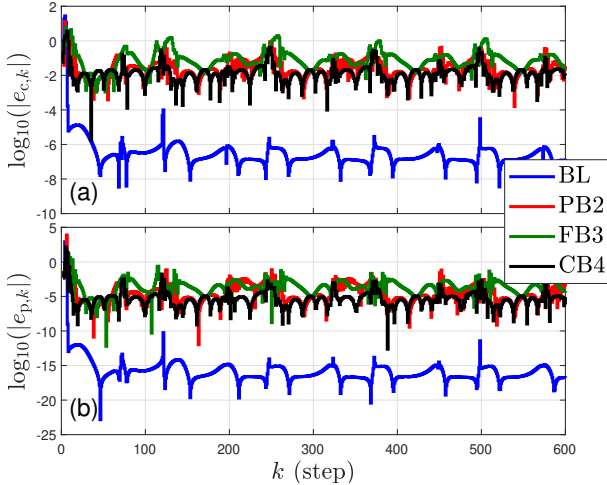


Fig. 6. Example 3: NPCAC of (58). (a) and (b) compare the command-following error $\log_{10}(|e_{c,k}|)$ and the one-step prediction error $\log_{10}(|e_{p,k}|)$, respectively, for BL, PB2, FB3, and CB4.

Example 4. Consider (1), where

$$F_1 \triangleq -1.1, \quad G_1(y_{k-1}) \triangleq 0.4 + 0.5 \sin(y_{k-1}), \quad (59)$$

which is equivalent to (58) except that atan is replaced with sin, in which case G_1 is not monotonic. For BL,

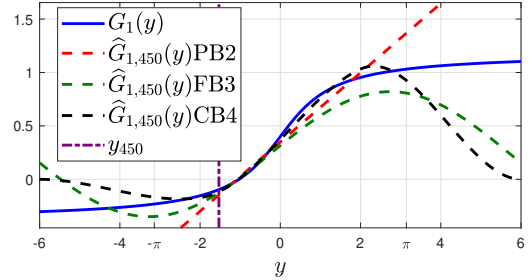


Fig. 7. Example 3: NPCAC of (58). The plot shows $G_1(y)$ and the estimate $\hat{G}_{1,450}(y)$ for BL, PB2, FB3, and CB4. Note that $\hat{G}_{1,450}(y)$ is accurate closer to y_{450} .

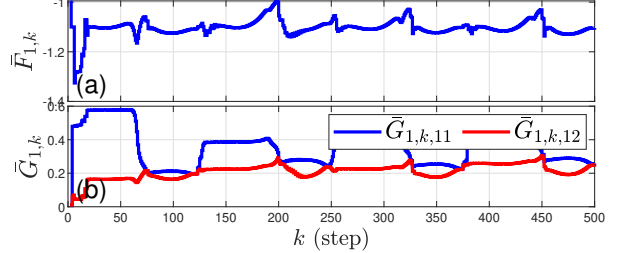


Fig. 8. Example 3: NPCAC of (58) for PB2. The plot shows the estimated coefficients $\bar{F}_{1,k}$ and $\bar{G}_{1,k}$ for PB2. Note that $\bar{G}_{1,k}$ for PB2 does not converge, indicating adaptation to $G_1(y_{k-1})$ at different step- k .

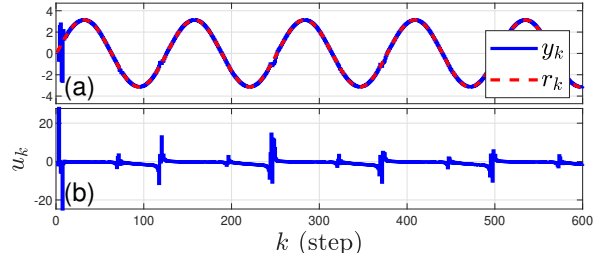


Fig. 9. Example 3: NPCAC of (58) for CB4. (a) shows the measurement y_k and the command r_k ; (b) shows the control u_k .

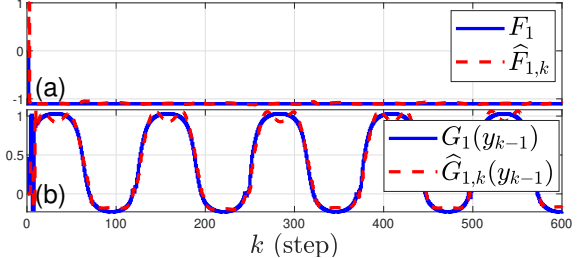


Fig. 10. Example 3: NPCAC of (58) for CB4. (a) shows F_1 and its estimate $\hat{F}_{1,k}$; (b) shows $G_1(y_{k-1})$ and its estimate $\hat{G}_{1,k}(y_{k-1})$.

we choose $g_1(y_{k-1}) = [1 \ \sin y_{k-1}]^T$. We set f_1 , $\bar{\theta}_0$, λ , R_0 , and R the same as Example 3. For PB2, we choose $R = 1$. We set f_1 , g_1 , $\bar{\theta}_0$, λ , and R_0 the same as Example 3. For FB3, we choose $R_0 = 1$ and $R = 4e-1$. We set f_1 , g_1 , L , $\bar{\theta}_0$, and λ the same as Example 3. For CB4, we choose $\lambda = 0.7$, $R_0 = 1e-1$, and $R = 8e-4$. We set $f_1 = 1$, g_1 , s_0 , s_3 , and $\bar{\theta}_0$ the same as Example 3.

Figure 11 compares the command-following error and the one-step prediction error for BL, PB2, FB3, and CB4. Figure 12 compares the estimated coefficient $\hat{G}_{1,450}(y)$

with $G_1(y)$ for BL, PB2, FB3, and CB4. Figure 13 shows the measurement y_k , the command r_k , and the control u_k for CB4. Figure 14 compares the estimated coefficients $\widehat{G}_{1,k}(y_{k-1})$ with $G_1(y_{k-1})$ for CB4. \diamond

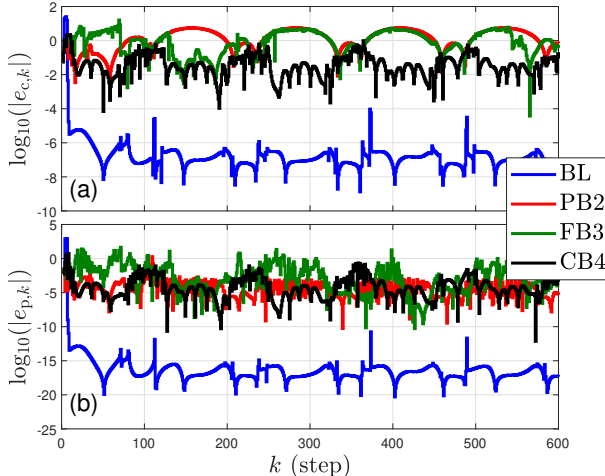


Fig. 11. Example 4: NPCAC of (59). (a) and (b) compare the command-following error $\log_{10}(|e_{c,k}|)$ and the one-step prediction error $\log_{10}(|e_{p,k}|)$, respectively, for BL, PB2, FB3, and CB4.

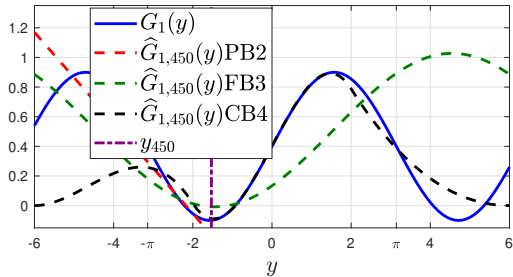


Fig. 12. Example 4: NPCAC of (59). The plot shows $G_1(y)$ and the estimate $\widehat{G}_{1,450}(y)$ for BL, PB2, FB3, and CB4. Note that $\widehat{G}_{1,450}(y)$ for CB4 is the most accurate closer to y_{450} . As a result, CB4 has the lowest command-following error in Figure 11.

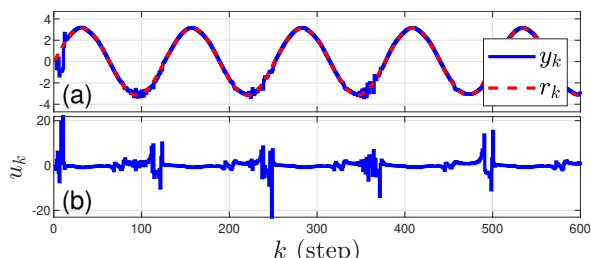


Fig. 13. Example 4: NPCAC of (59) for CB4. (a) shows the measurement y_k and the command r_k ; (b) shows the control u_k .

Figure 11 shows that the performance for CB4 is better than FB3. In the next example, we increase FB3 to FB5.

Example 5. Consider (59). For BL, PB2, and CB4, we set f_1 , g_1 , R_0 , $\bar{\theta}_0$, λ , and R the same as Example 4. For FB5, we choose $g_1(y_{k-1}) = b_{F,2}(y_{k-1})$, $R_0 = 1$, and $R = 4e-1$. We set f_1 , L , $\bar{\theta}_0$, and λ the same as Example 4.

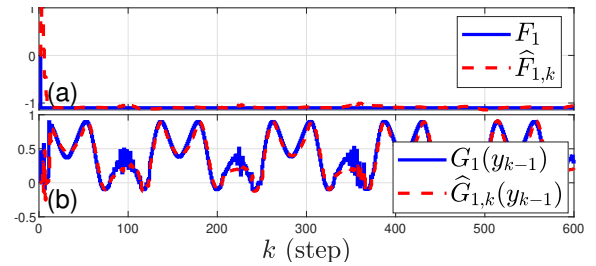


Fig. 14. Example 4: NPCAC of (59) for CB4. (a) shows F_1 and its estimate $\widehat{F}_{1,k}$; (b) shows $G_1(y_{k-1})$ and its estimate $\widehat{G}_{1,k}(y_{k-1})$.

Figure 15 compares the command-following error and the one-step prediction error for BL, PB2, FB5, and CB4. Figure 16 compares the estimated coefficient $\widehat{G}_{1,450}(y)$ with $G_1(y)$ for BL, PB2, FB5, and CB4. Figure 17 shows the measurement y_k , the command r_k , and the control u_k for FB5. Figure 18 compares the estimated coefficients $\widehat{G}_{1,k}(y_{k-1})$ with $G_1(y_{k-1})$ for FB5. \diamond

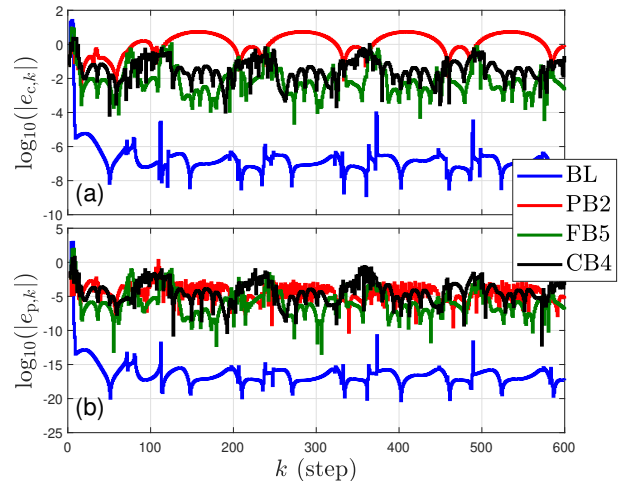


Fig. 15. Example 5: NPCAC of (59). (a) and (b) compare the command-following error $\log_{10}(|e_{c,k}|)$ and the one-step prediction error $\log_{10}(|e_{p,k}|)$, respectively, for BL, PB2, FB5, and CB4.

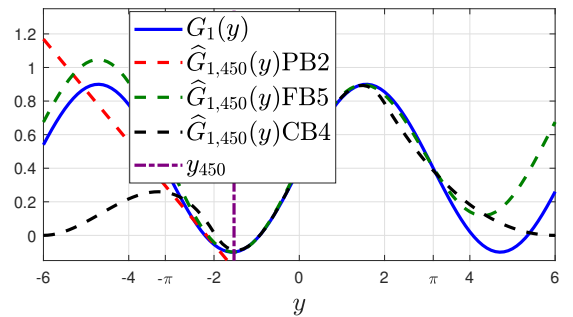


Fig. 16. Example 5: NPCAC of (59). The plot shows $G_1(y)$ and the estimate $\widehat{G}_{1,450}(y)$ for BL, PB2, FB5, and CB4. Note that $\widehat{G}_{1,450}(y)$ for FB5 is the most accurate closer to y_{450} compared to Figure 12. As a result, FB5 has the lowest command-following error in Figure 15.

Figure 15 of Example 5 shows an improved performance for FB5 compared to Figure 11 of Example 4 FB3.

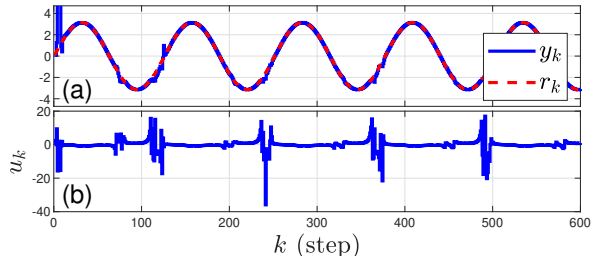


Fig. 17. Example 5: NPCAC of (59) for FB5. (a) shows the measurement y_k and the command r_k ; (b) shows the control u_k .

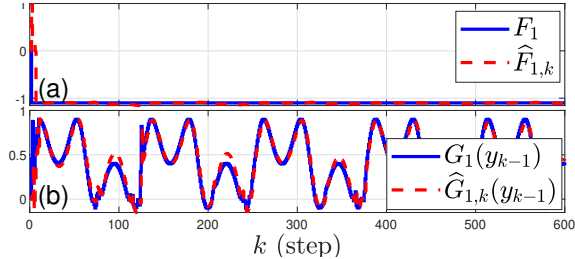


Fig. 18. Example 5: NPCAC of (59) for FB5. (a) shows F_1 and its estimate $\hat{F}_{1,k}$; (b) shows $G_1(y_{k-1})$ and its estimate $\hat{G}_{1,k}(y_{k-1})$.

VIII. Conclusions and Future Research

The numerical investigation in this paper is a first step aimed at adaptive nonlinear model predictive control, where all learning is performed online without prior modeling, training, or data collection. For a chosen set of basis functions, online system identification uses a pseudo-linear, input-output model that is linear in parameters and thus amenable to RLS with SIFT.

The numerical results in this paper reveal that good command-following performance can be obtained without identifying a highly accurate model. This observation is consistent with LPCAC, where the identified model is often sufficient for the control objective but rarely accurate at all frequencies [19].

Future research will focus on several fundamental and practical issues. First, we will examine the performance of this method on higher-order nonlinear systems. Next, we will investigate alternative basis functions to determine their effectiveness. Furthermore, extension to MIMO systems is a key challenge, where the basis functions are needed for vector arguments. Next, we will apply NPCAC to physically motivated sampled-data systems that are not necessarily in the form of pseudo-linear input-output models. Finally, all of these investigations can benefit from more efficient and more accurate nonlinear model predictive control methods.

References

- [1] T. Samad and et al, "Industry engagement with control research: Perspective and messages," *Ann. Rev. Contr.*, vol. 49, pp. 1–14, 2020.
- [2] W. H. Kwon and A. E. Pearson, "On feedback stabilization of time-varying discrete linear systems," *IEEE Trans. Autom. Contr.*, vol. AC-23, no. 3, pp. 479–481, 1978.
- [3] S. S. Keerthi and E. G. Gilbert, "Optimal infinite-horizon feedback laws for a general class of constrained discrete-time systems: Stability and moving-horizon approximations," *J. Opt. Theory App.*, vol. 57, no. 2, pp. 265–293, 1988.
- [4] W. Kwon and S. Han, *Receding Horizon Control: Model Predictive Control for State Models*. Springer, 2006.
- [5] E. F. Camacho and C. Bordons, *Model Predictive Control*, 2nd ed. Springer, 2007.
- [6] J. B. Rawlings, D. Q. Mayne, and M. M. Diehl, *Model Predictive Control: Theory, Computation, and Design*, 2nd ed. Nob Hill, 2017.
- [7] M. Morari and J. H. Lee, "Model predictive control: past, present and future," *Computers Chem. Engin.*, vol. 23, no. 4, pp. 667–682, 1999.
- [8] U. Eren, A. Prach, B. B. Koçer, S. V. Raković, E. Kayacan, and B. Açıkmese, "Model predictive control in aerospace systems: Current state and opportunities," *J. Guid. Cont. Dyn.*, vol. 40, no. 7, pp. 1541–1566, 2017.
- [9] J. A. Andersson, J. Gillis, G. Horn, J. B. Rawlings, and M. Diehl, "Casadi: a software framework for nonlinear optimization and optimal control," *Math. Progr. Comp.*, vol. 11, pp. 1–36, 2019.
- [10] M. Wright, "The interior-point revolution in optimization: history, recent developments, and lasting consequences," *Bull. Amer. Math. Soc.*, vol. 42, pp. 39–56, 2005.
- [11] P. T. Boggs and J. W. Tolle, "Sequential quadratic programming," *Acta Numerica*, vol. 4, pp. 1–51, 1995.
- [12] P. E. Gill and E. Wong, "Sequential quadratic programming methods," in *Mixed Integer Nonlinear Prog.* Springer, 2012, pp. 147–224.
- [13] P. S. G. Cisneros, S. Voss, and H. Werner, "Efficient nonlinear model predictive control via quasi-lpv representation," in *2016 IEEE 55th Conference on Decision and Control (CDC)*, 2016, pp. 3216–3221.
- [14] C. Hespe and H. Werner, "Convergence properties of fast quasi-lpv model predictive control," in *2021 60th IEEE Conference on Decision and Control (CDC)*, 2021, pp. 3869–3874.
- [15] D. W. Clarke, C. Mohtadi, and P. S. Tuffs, "Generalized Predictive Control—Part I. The Basic Algorithm," *Automatica*, vol. 23, pp. 137–148, 1987.
- [16] ———, "Generalized Predictive Control—Part I. Equations and Interpretations," *Automatica*, vol. 23, pp. 149–160, 1987.
- [17] R. Bitmead, M. Gevers, and V. Wertz, *Adaptive Optimal Control: The Thinking Man's GPC*. New York: Prentice Hall, 1990.
- [18] E. Mosca, *Optimal, Predictive, and Adaptive Control*. Prentice Hall, 1995.
- [19] T. W. Nguyen, S. A. U. Islam, D. S. Bernstein, and I. V. Kolmanovsky, "Predictive Cost Adaptive Control: A Numerical Investigation of Persistency, Consistency, and Exigency," *IEEE Contr. Sys. Mag.*, vol. 41, pp. 64–96, December 2021.
- [20] A. Mesbah, "Stochastic model predictive control with active uncertainty learning: A survey on dual control," *Ann. Rev. Contr.*, vol. 45, pp. 107–117, 2018.
- [21] M. Kamaldar, N. Mohseni, S. A. U. Islam, and D. S. Bernstein, "A Numerical and Experimental Investigation of Predictive Cost Adaptive Control for Noise and Vibration Suppression," *Mech. Sys. Sig. Proc.*, vol. 221, pp. 1–42, 2024.
- [22] R. J. Richards, J. A. Marshall, and D. S. Bernstein, "Experimental flight testing a quadcopter autopilot based on predictive cost adaptive control," in *Proc. Amer. Contr. Conf.*, 2025, pp. 2471–2476.
- [23] R. J. Richards, S. A. U. Islam, and D. S. Bernstein, "Predictive cost adaptive control of the nasa benchmark flutter model," *AIAA J. Guid. Contr.*, pp. 1–17, 2025, available online.
- [24] S. A. U. Islam and D. S. Bernstein, "Adaptive flight control of an f-16 without prior modeling," *AIAA J. Guid. Contr.*, pp. 1–18, 2025, available online.
- [25] M. O. Williams, I. G. Kevrekidis, and C. W. Rowley, "A data-driven approximation of the koopman operator: Extending dynamic mode decomposition," *Journal of nonlinear science*, vol. 25, no. 6, p. 1307–1346, 2015.
- [26] H. M. Calderón, E. Schulz, T. Oehlschlägel, and H. Werner, "Koopman operator-based model predictive control with re-

cursive online update,” in 2021 European Control Conference (ECC), 2021, pp. 1543–1549.

[27] M. Korda and I. Mezić, “Linear predictors for nonlinear dynamical systems: Koopman operator meets model predictive control,” *Automatica*, vol. 93, pp. 149–160, 2018.

[28] M. Kamaldar and D. S. Bernstein, “Output-feedback nonlinear model predictive control with iterative state- and control-dependent coefficients,” arXiv:2309.11589, 2023.

[29] R. A. Alhazmi, J. A. Paredes, S. A. U. Islam, and D. S. Bernstein, “Application of root-finding methods to iterative model predictive control of pseudo-linear systems,” in Proc. Amer. Contr. Conf., 2025, pp. 3385–3390.

[30] L. Balbis, R. Katebi, R. Dunia, A. Ordys, and M. J. Grimble, “Nonlinear predictive control for real time applications,” in 2006 IEEE Conference on Computer Aided Control System Design, 2006 IEEE International Conference on Control Applications, 2006 IEEE International Symposium on Intelligent Control, 2006, pp. 211–216.

[31] B. Lai and D. S. Bernstein, “Sift-rls: Subspace of information forgetting recursive least squares,” 2024. [Online]. Available: <https://arxiv.org/abs/2404.10844>

[32] R. Alhazmi, S. A. U. Islam, and D. Bernstein, “Nonlinear model predictive guidance for 6dof pursuer/evader engagements,” in AIAA SCITECH Forum, 2025.